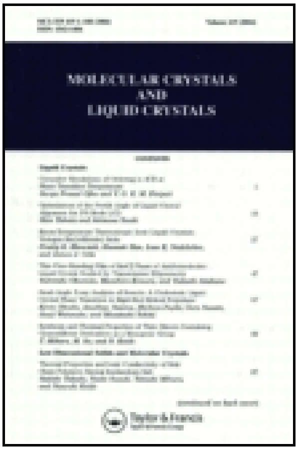

Molecular Crystals and Liquid Crystals
Publication details, including instructions for authors and subscription information:
http://www.tandfonline.com/loi/gmcl16

Studies on Binary Mixtures of Systems Which Exhibit a Maximum as Well as a Minimum in the A-N Transition Boundary

B. S. Srikanta [a] & N. V. Madhusudana [a]
[a] Raman Research Institute, Bangalore, 560080, India

To cite this article: B. S. Srikanta & N. V. Madhusudana (1983): Studies on Binary Mixtures of Systems Which Exhibit a Maximum as Well as a Minimum in the A-N Transition Boundary, Molecular Crystals and Liquid Crystals, 99:1, 203-221

To link to this article: http://dx.doi.org/10.1080/00268948308072043

Mol. Cryst. Liq. Cryst., 1983, Vol. 99, pp. 203–221
0026-8941/83/9904–0203/$18.50/0

Studies on Binary Mixtures of Systems Which Exhibit a Maximum as Well as a Minimum in the A–N Transition Boundary[†]

B. S. SRIKANTA and N. V. MADHUSUDANA
Raman Research Institute, Bangalore 560080, India

(Received February 23, 1983)

We have studied the binary phase diagrams of (I) p′-nitrophenyl-p-*n*-octyloxybenzoate with (2-hydroxy)-p-ethoxybenzylidene-p′-butylaniline, and (II) p′-*n*-octyloxy-p-cyanobiphenyl with p-butoxyphenyl-(p′-pentyloxy)benzoate. Both of them show a strong maximum in the A–N boundary, indicative of an induced A phase, and further, a well defined minimum for a composition rich in the highly polar component. The interactions responsible for the induced phase are much stronger for the system II than for the system I. We have investigated the temperature variations of the layer spacings for various compositions of both the systems. In system I, there is a considerable thermal expansion of the spacing, the expansion coefficient attaining a maximum value for the composition corresponding to the minimum in the A–N boundary. We have given a physical interpretation of this observation. The dielectric anisotropies of various compositions of system I have also been investigated and their temperature dependences interpreted in terms of the physical model mentioned above. The conductivity anisotropy changes sign for all compositions exhibiting the A phase. The temperature of crossover in relation to T_{AN} is the highest for the mixture which exhibits the minimum value of T_{AN}, since the A–N transition is almost of a second order character for this composition.

INTRODUCTION

There have been a large number of studies on the binary phase diagrams of mixtures which exhibit the induced A phase.[1-10] Such a phase is observed in some composition range of the mixtures when one of the components has the strongly polar cyano or nitro end group while the other component has

---

[†] Presented at the Ninth International Liquid Crystal Conference, Bangalore, 1982.

no such group. Thus permanent dipole-induced dipole interactions appear to be important for the occurrence of the induced phase. Further, there is experimental evidence that a charge transfer complex formation takes place between the molecules of the two kinds, the highly polar component acting as the acceptor while the other component acts like a donor.[11,12] This interaction appears to lead to the formation of a layered arrangement characteristic of smectic phases.

If the highly polar compound itself exhibits a smectic A phase, it will be of a bilayer variety, the layer spacing being considerably larger than the molecular length.[13] The bilayer arises due to the strong antiparallel correlations between the neighboring molecules of compounds with terminal polar groups.[14] In binary mixtures of such compounds with weakly polar compounds, it is found in some cases that the bilayer smectic is immiscible with the induced A phase.[15] If the bilayer corresponds to nearly two molecular lengths (A_2 phase), one gets a phase transition between the A_2 phase and induced A phase which is an A_1, i.e., a monolayer phase.[16]

We report in this paper the phase diagrams of two systems, both of which exhibit a maximum as well as a minimum in the A–N transition boundary. The interactions responsible for the formation of the induced A phase are much stronger in one system than in the other, as revealed by the phase diagrams. This results in a perceptible difference in the thermal evolution of layer spacing between the two systems for compositions lying close to the minimum in the AN boundary. We also report dielectric and conductivity studies on one of the systems.

EXPERIMENTAL

The transition temperatures were determined by using a Mettler hot stage (FP-52) in conjunction with a polarizing microscope. They were also confirmed using a differential scanning calorimeter (Perkin Elmer DSC-2). The X-ray studies were made on samples taken in Lindemann capillary tubes and aligned by slowly cooling in a magnetic field of strength 4 KGauss. Nickel filtered copper $K\alpha$ radiation was used for the purpose and the diffracted beams were recorded photographically. The principal dielectric constants and conductivities were determined using a Wayne Kerr bridge (B642) which operates at 1592 Hz. For this purpose, a 125 μ thick sample was taken between two tin oxide coated plates and aligned in the required direction by slowly cooling in a 14 KGauss strong magnetic field.

RESULTS AND DISCUSSION

The two binary systems investigated are: (I) p′-nitro-phenyl-p-*n*-octyloxybenzoate (NPOOB) with (2-hydroxy)-p-ethoxy-benzylidene-p′-butylaniline (OH-EBBA) and (II) p′-*n*-octyloxy-p-cyanobiphenyl (8 OCB) with p-butoxyphenyl-(p′-pentyloxy)benzoate (40.05). 8 OCB was bought from Hoffmann-La Roche, 40.05 and OH-EBBA were synthesized in our chemistry laboratory and the NPOOB sample was kindly sent to us by Prof. A. C. Griffin.

The structural formula of all the compounds are shown in Figure 1. NPOOB and 8 OCB have the strongly polar nitro and cyano end groups respectively, and both of them exhibit the A phase. The phase diagrams of the two systems are shown in Figures 2 and 3 respectively. Both the phase diagrams exhibit a pronounced maximum in the AN boundary, indicative of induced A phase, and further, a well defined minimum for a composition rich in the highly polar component. It is clear that in system II, the tendency to form the induced phase is much stronger: the A phase exists up to very high temperatures and near the peak, it transforms directly to the isotropic phase. On the other hand, the peak in the induced A–N phase boundary of system I is much less pronounced and lies well below the NI transition

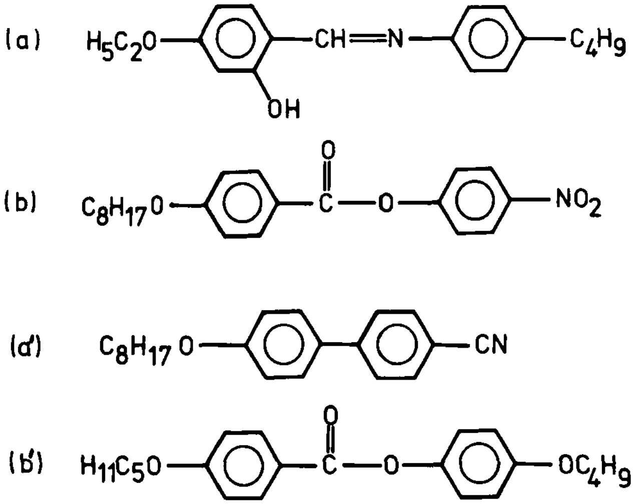

FIGURE 1 Structural formulae of (a) (2-hydroxy)-p-ethoxy-benzylidene-p′-butylaniline (OH-EBBA), (b) p′-nitro-phenyl-p-*n*-octyloxybenzoate (NPOOB), (a′) p′-*n*-octyloxy-p-cyanobiphenyl (8 OCB) and (b′) p-butoxy-phenyl-p′-pentyloxybenzoate (40.05).

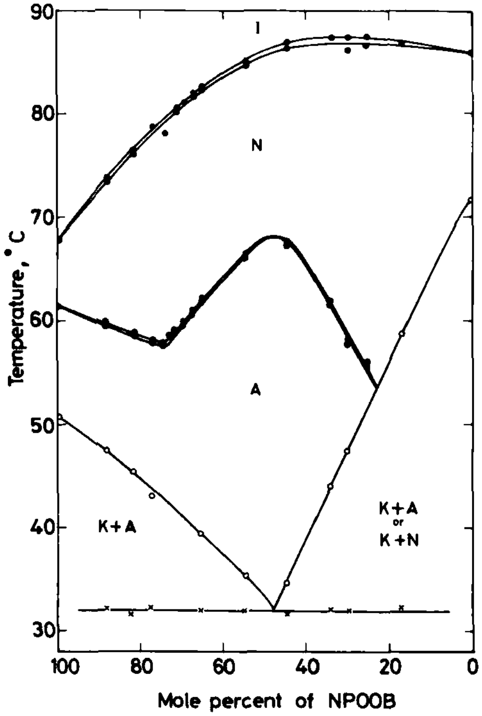

FIGURE 2 Phase diagram of mixtures of NPOOB with OH-EBBA (system I). *K* stands for the crystalline phase.

boundary. This means that the interactions responsible for the induction of the A phase are much stronger in system II than in system I. The induced A phase also influences the NI transition boundary as can be easily seen in Figures 2 and 3.

The entropy of transition as a function of concentration of system I is shown in Figure 4. It is interesting to note that the shape of this curve is very similar to that of T_{AN}, exhibiting a maximum for a composition which also exhibits the maximum in the phase boundary. Further, the A–N transition has almost a second order character for the composition exhibiting the minimum in the phase boundary. A very similar trend is found even for the system II, the entropy of the A–I transition near the maximum (see Figure 3) being very much larger than the highest value of system I. This once again shows that the interactions responsible for the induced smectic phase in system II are much stronger than in system I.

The temperature variations of the layer spacings (*d*) are shown in Figures 5 and 6 for various compositions of systems I and II respectively. The

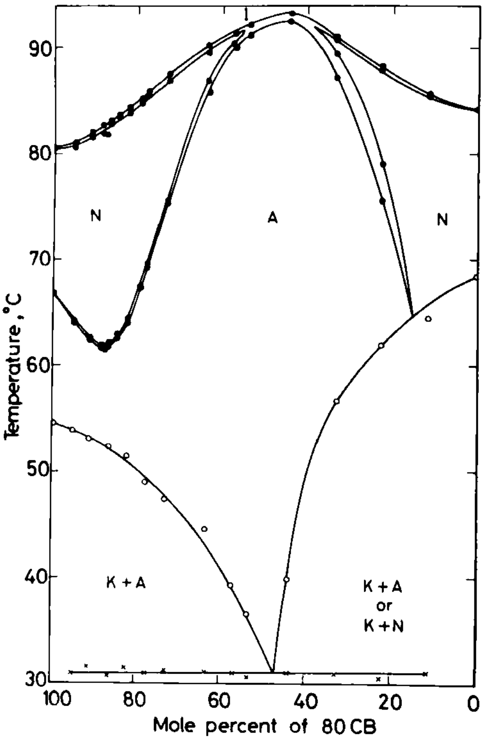

FIGURE 3 Phase diagram of mixtures of 8 OCB with 40.05 (system II). *K* stands for the crystalline phase.

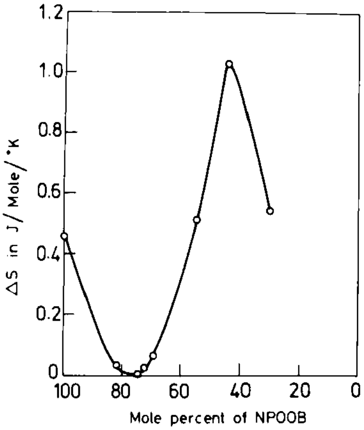

FIGURE 4 The entropy of the *A*–*N* transition of system I as a function of composition.

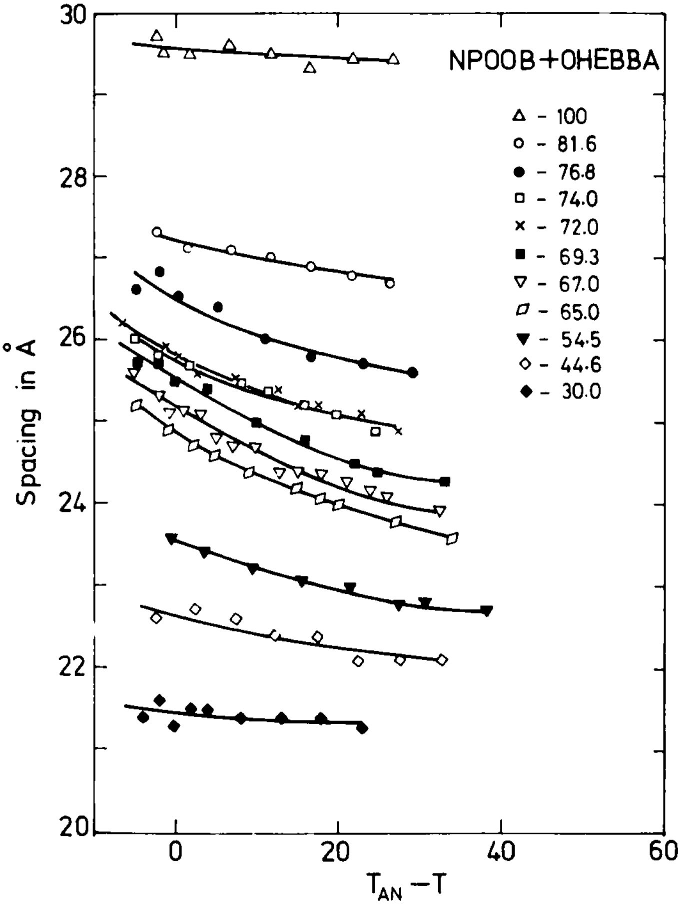

FIGURE 5 Layer spacings of mixtures of NPOOB with OH-EBBA as functions of (T_{AN} − T). The numbers against different symbols indicate the mole percentage of NPOOB.

molecular lengths of the four compounds calculated using Dreiding models are 24.0 Å (NPOOB), 20.2 Å (OH-EBBA), 22.5 Å (8 OCB) and 24.9 Å (40.05). Using these data, the layer spacings for compositions rich in the weakly polar component correspond to appropriate average molecular lengths (l) of the components, i.e., such compositions consist of only the monolayer species. On the other hand, compositions rich in the strongly polar component have both monolayer and bilayer species, in agreement with results on other systems.[15] Calculations at $T_{AN} - T = 2.5°$ show that the (d/l) ratio varies smoothly from a value <1 for the weakly polar component to ~1.23 in the case of pure NPOOB in system I and to ~1.42

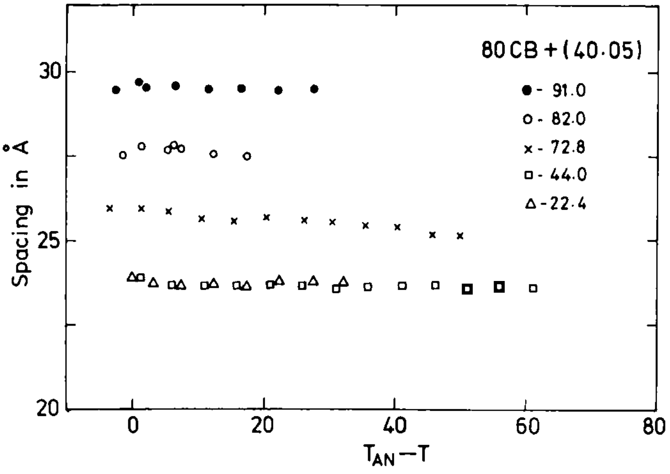

FIGURE 6 Layer spacings of mixtures of 8 OCB with 40.05 as functions of $(T_{AN} - T)$. The numbers indicate the mole percentage of 8 OCB.

in the case of 8 OCB in system II. The *d* values of NPOOB and 8 OCB agree with earlier measurements[17,13] and the smectic phases exhibited by them can be classified as A_d.[18]

We did not find any evidence of an A_d–A_1 transition in our X-ray studies on the two systems. The well defined minima in the phase diagrams indicate that the A_d and A_1 (i.e., induced smectic) phases may not be structurally compatible. However, the coexistence of both the bimolecular and monomolecular species for compositions close to the minima, as indicated by the X-ray studies, appears to smear out any possible A_d–A_1 transition.

We notice from Figure 5 that the thermal expansion coefficient of the layer spacing of system I increases as we approach a composition corresponding to the minimum in the AN boundary from either side. This is brought out clearly in Figure 7. Further, the expansion coefficient increases with increase of temperature for any given composition in this region (Figure 5). On the other hand, such a trend is not very conspicuous in system II (Figure 6). We believe that the large expansion of the layer spacing of system I for compositions close to the minimum is not connected with the nearly second order character of the A–N transition for these mixtures. First, such a trend has not been reported in any single component system, and further, system II does not exhibit this trend, even though the A–N transition is of nearly second order character close to the minimum in this case also. We attribute this difference in behavior between the two systems to the large difference in the strengths of intermolecular inter-

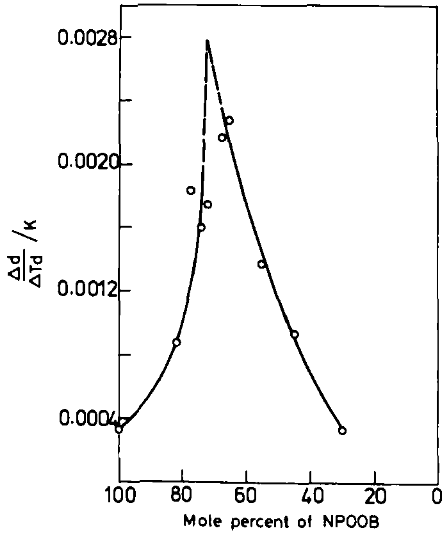

FIGURE 7 The thermal expansion coefficients of the layer spacings of mixtures of NPOOB with OH-EBBA at $T_{AN} - T = 2.5°$.

actions between the components in the two cases. As we discussed earlier, the interaction energy between the strongly polar and weakly polar molecules is relatively weak in system I, and perhaps only slightly higher than the interaction energy which gives rise to antiparallel correlation between two neighboring NPOOB molecules. Consequently, as the temperature is increased, the strongly polar-weakly polar pairs can easily break up allowing NPOOB molecules to form more antiparallel pairs and thus the thermal expansion coefficient can be very large. It can also be noted that for compositions near the minimum, there are three NPOOB molecules for every OH-EBBA molecule. Further, for these compositions the A_d and A_1 (i.e., induced smectic) structures coexist and the thermal expansion coefficient attains large values.

The principal dielectric constants ($\varepsilon_\parallel$ and $\varepsilon_\perp$) and the mean values ($\bar{\varepsilon}$) are shown for some representative compositions of system I in Figures 8–12. In the case of NPOOB (Figure 8) both $\varepsilon_\parallel$ and $\varepsilon_\perp$ show a decrease as the sample is cooled across T_{AN}. The values are in broad agreement with earlier measurements on this compound.[19,20] NPOOB has a weakly first order AN transition (Figure 4) and the increase of $\varepsilon_\parallel$ and decrease of $\varepsilon_\perp$ as the sample is cooled in the A phase probably means that the antiparallel correlations do not vary much with temperature in the A phase. The $\bar{\varepsilon}$ value increases with temperature in the N phase, indicating a corresponding decrease of the antiparallel correlations. It is interesting to note that in the mixture containing 74% NPOOB (Figure 9) which is the composition exhibiting the mini-

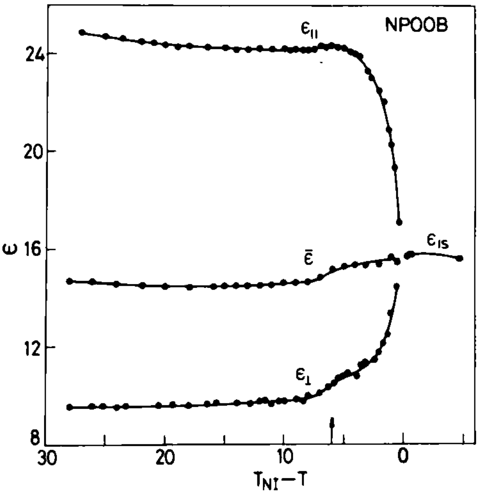

FIGURE 8 Dielectric constants of NPOOB as functions of relative temperature. In this and the following diagrams, a vertical arrow on the temperature axis indicates T_{AN}.

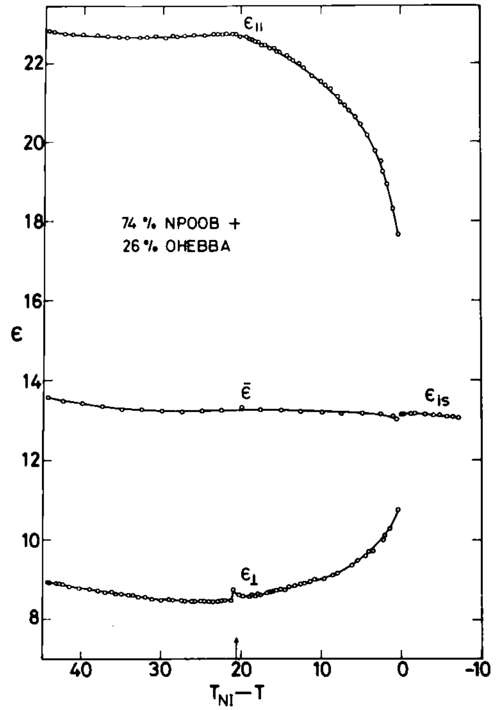

FIGURE 9 Dielectric constants of a mixture of 74% NPOOB with 26% OH-EBBA as functions of relative temperature.

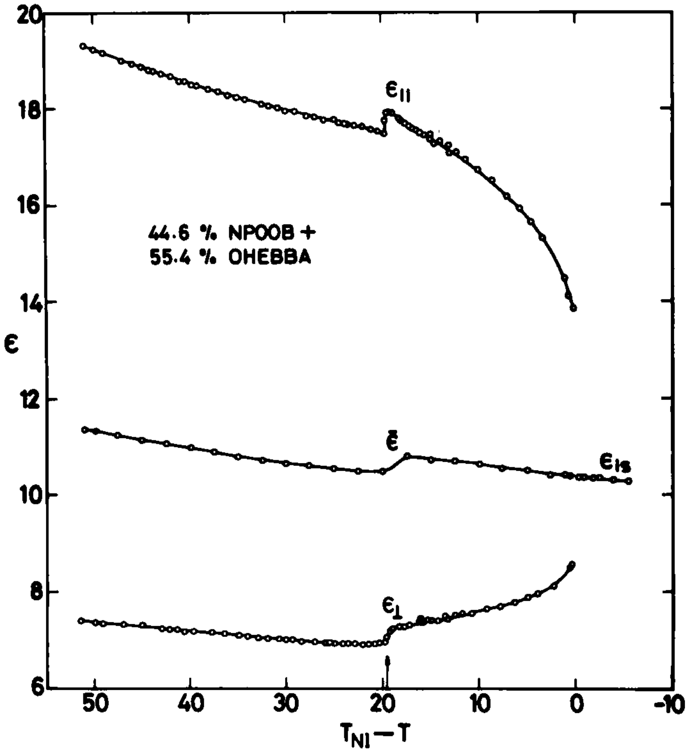

FIGURE 10 Dielectric constants of a mixture of 44.6% NPOOB with 55.4% OH-EBBA as functions of relative temperature.

mum in the A–N boundary, $\varepsilon_{\perp}$ increases with decrease of temperature in the A phase. This can be easily understood in terms of the increase of the number of strongly polar-weakly polar molecular pairs at the expense of the antiparallel strongly polar molecular pairs. Assuming that charge transfer complexes are forming, it is clear that $\varepsilon_{\perp}$ should increase. The cusp-like peak observed in $\varepsilon_{\perp}$ near T_{AN} arises from the strong tendency of the director to orient homeotropically for these compositions.[21] For compositions close to the maximum in the phase boundary (Figure 10), we see quite a strong reduction in both $\varepsilon_{\parallel}$ and $\varepsilon_{\perp}$ as the sample is cooled across T_{AN}. This may be attributed to the fact the heat of A–N transition is quite large for this composition (Figure 4) and the orientational order parameter can be expected to jump to a higher value in the A phase. The decrease in $\varepsilon_{\parallel}$ probably arises partly from an increase in the antiparallel correlations of the NPOOB molecular pairs and partly due to the tendency of the director to prefer a homogeneous alignment in this composition range. However, the strongly

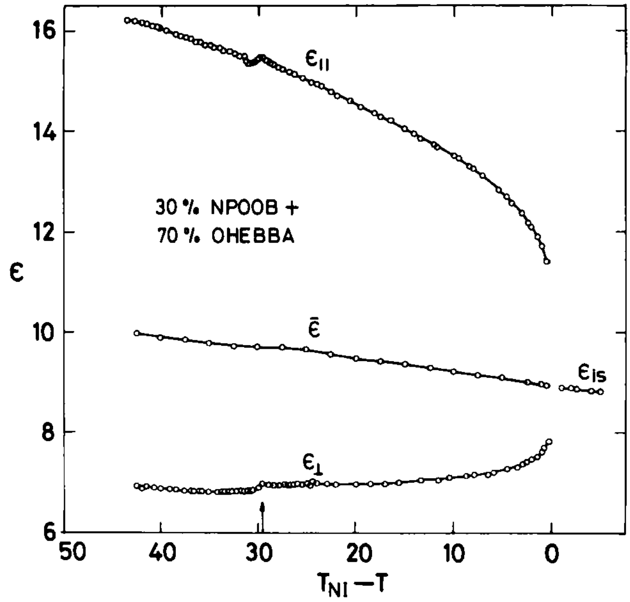

FIGURE 11 Dielectric constants of a mixture of 30% NPOOB with 70% OH-EBBA as functions of relative temperature.

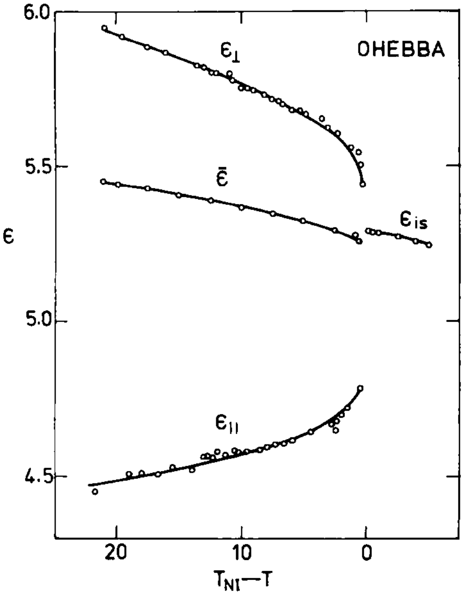

FIGURE 12 Dielectric constants of OH-EBBA as functions of relative temperature.

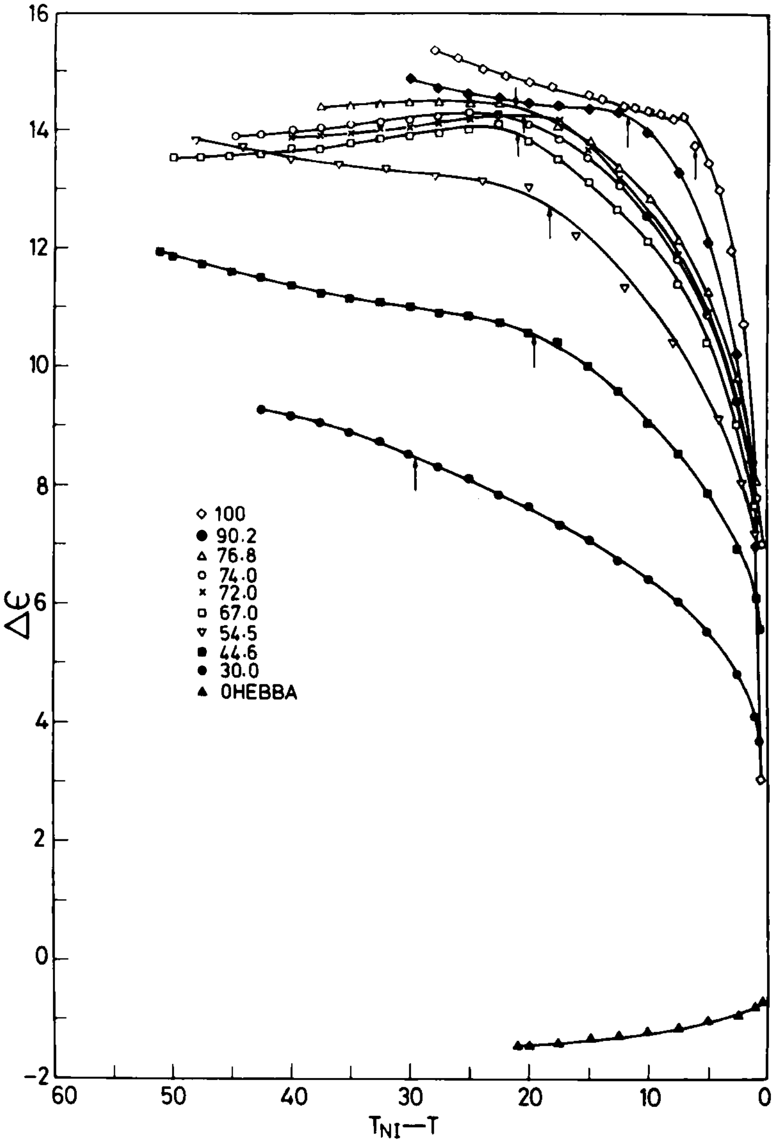

FIGURE 13 Dielectric anisotropies of mixtures of NPOOB with OH-EBBA as functions of relative temperature. The numbers indicate mole percentages of NPOOB and the arrows indicate T_{AN}.

polar-weakly polar molecular pairs should be very large for this composition which is close to the maximum in the phase boundary, and the permanent dipole moments of the individual NPOOB molecules belonging to such pairs fully contribute to $\varepsilon_{\parallel}$ unlike in the case of pairs of antiparallel NPOOB molecules in which there is partial compensation of the dipole moment. Further, the charge transfer complex pairs increase with decrease of temperature. Thus $\varepsilon_{\parallel}$ increases substantially as the temperature is lowered in the A phase. $\varepsilon_{\perp}$ also increases with decrease of temperature as already discussed for the composition having a higher concentration of NPOOB.

With a further decrease of NPOOB concentration (Figure 11), the effects observed for the 44.6% NPOOB mixture get less pronounced and indeed understandably, the increase of $\varepsilon_{\perp}$ with lowering of temperature becomes weak. OH-EBBA itself has a negative dielectric anisotropy (Figure 12).

The dielectric anisotropies of all the systems that we have studied are collected in Figure 13. It is quite clear that the temperature variation of $\Delta\varepsilon$ in the A phase is quite different for compositions close to the minimum in the AN boundary compared to those close to the maximum. The anisotropy *decreases* as the temperature is decreased in the A phase for compositions close to the minimum for reasons discussed earlier. On the other hand, for compositions close to the maximum in the A–N boundary, $\Delta\varepsilon$ *increases*

TABLE I

Comparison of the measured and calculated values of $\Delta\varepsilon$ and $\bar{\varepsilon}$ of various mixtures at $T_{NI} - T = 20°$

Mole per cent of NPOOB	Calculated value		Measured value		Ratio of measured to calculated values	
	$\Delta\varepsilon$	$\bar{\varepsilon}$	$\Delta\varepsilon$	$\bar{\varepsilon}$	$R(\Delta\varepsilon)$	$R(\bar{\varepsilon})$
100	—	—	14.80	14.41	—	—
90.2	13.22	13.52	14.45	13.90	1.09	1.03
76.8	11.03	12.32	14.30	13.50	1.30	1.09
74.0	10.58	12.07	14.10	13.25	1.33	1.10
72.0	10.25	11.89	14.20	13.35	1.39	1.12
67.0	9.44	11.44	13.80	12.80	1.46	1.12
54.5	7.41	10.32	12.85	11.70	1.73	1.13
44.6	5.80	9.44	10.55	10.50	1.82	1.11
30.0	3.43	8.13	7.60	9.50	2.22	1.17
OH-EBBA	—	—	−1.45	5.44	—	—

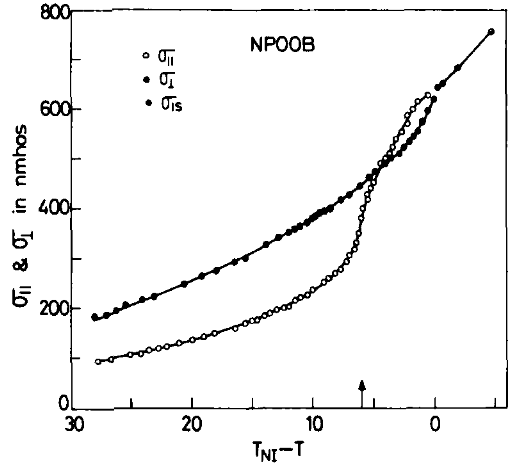

FIGURE 14 Principal conductivities of NPOOB as functions of relative temperature.

with decrease of temperature. We may also point out two unusual features: (i) the mixture with 74% NPOOB has a lower value of $\Delta\varepsilon$ than that of the mixture with 72% NPOOB in the nematic phase close to T_{AN}; (ii) because of the opposite variation of $\Delta\varepsilon$ with temperature in the A phase of the mixture with 54.5% NPOOB compared with mixtures with higher percentages of NPOOB, at sufficiently low temperatures, the former has *higher* $\Delta\varepsilon$ values than many mixtures of the latter type.

It is also interesting to compare the measured values of $\Delta\varepsilon$ and $\bar{\varepsilon}$ of the mixtures with the corresponding numbers calculated on the basis of an additive law of the type $\Delta\varepsilon_{\text{mix}} = P_1\,\Delta\varepsilon_1 + P_2\,\Delta\varepsilon_2$ where P_1 is the mole fraction of the first component, etc. The results are shown in Table I.

It is clear that $(\Delta\varepsilon_{\text{meas}}/\Delta\varepsilon_{\text{calc}})$ is larger than one in agreement with some earlier observations,[4] and increases with increasing percentage of OH-EBBA. This is mainly because the probability of breaking up of antiparallel associations between NPOOB molecules increases with increasing percentage of OH-EBBA molecules. Consequently, the NO_2 group can more effectively contribute to $\varepsilon_{\parallel}$. As can be easily seen from Figures 8–12, $\varepsilon_{\parallel}$ of mixtures is much higher than what an additive law to that parameter would have given. The $\varepsilon_{\perp}$ value does not change very much between NPOOB and OH-EBBA and hence does not contribute much to the deviation of the above ratio from 1. $(\bar{\varepsilon}_{\text{meas}}/\bar{\varepsilon}_{\text{calc}})$ shows values which are >1 by ~10–20%.

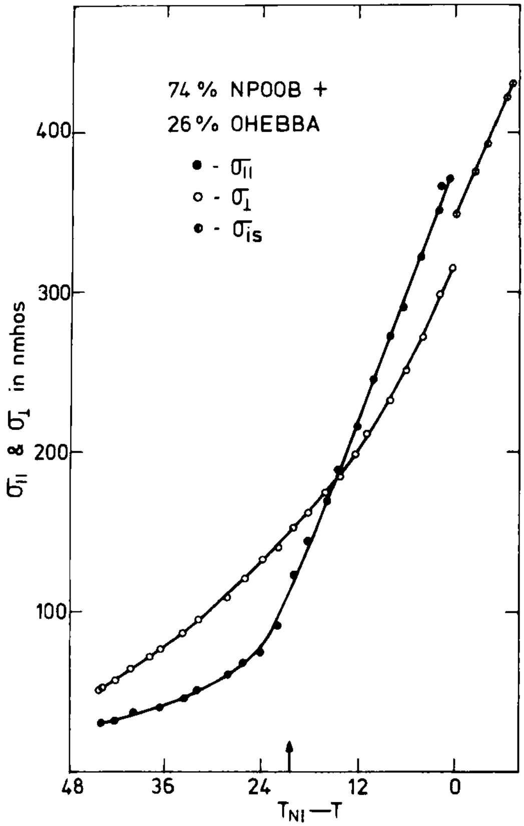

FIGURE 15 Principal conductivities of a mixture of 74% NPOOB with 26% OH-EBBA as functions of relative temperature.

The principal conductivities of three representative compositions are shown in Figures 14–16. In all the cases, as the sample is cooled, the conductivity anisotropy changes sign, becoming negative a few degrees above T_{AN} as is to be expected.[22] $\sigma_{\parallel}$ shows a 'jump' at T_{AN} for both NPOOB (Figure 14) and the mixture with 44.6% NPOOB (Figure 16). This is caused by the fact that the A–N transition has a first order character in both the cases (Figure 4). On the other hand, $\sigma_{\parallel}$ falls steeply up to T_{AN} in the case of the mixture with 74% NPOOB and then levels off in the A phase (Figure 15), since the A–N transition in this case is almost of second order character. It is interesting to note that $\sigma_{\perp}$ varies smoothly across T_{AN} for all

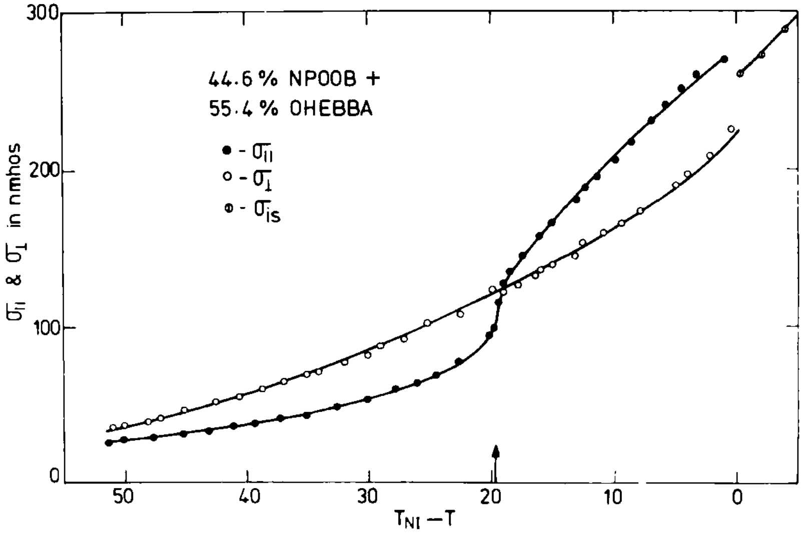

FIGURE 16 Principal conductivities of a mixture of 44.6% NPOOB with 55.4% OH-EBBA as functions of relative temperature.

the compositions studied. The temperature variations of the conductivity ratio $\sigma_R = \sigma_{\parallel}/\sigma_{\perp}$ are shown for all the systems studied in Figure 17. The diagram is somewhat complicated, mainly because of the peculiar shape of the A–N boundary (Figure 2). Further, it is known that σ_R depends on the nature and concentration of the conducting impurities, the value of σ_R going up if the medium has higher conductivity.[23,24] The conducting impurities in our samples are unknown, and in Figure 17 we have shown the values of the mean specific conductivity $\overline{K}$ at a common temperature for all the systems studied. $\overline{K} = (l'/A)\overline{\sigma}$ where l'/A the geometrical parameter of the cell was determined from the measured value of the capacitance of the empty cell and $\overline{\sigma}$ is the measured conductivity if the medium is in the isotropic phase, or $\overline{\sigma} = (\sigma_{\parallel} + 2\sigma_{\perp})/3$ if it is in the nematic phase. It is clear that NPOOB has a much higher value of $\overline{K}$ than OH-EBBA, the mixtures having some intermediate values. Nevertheless, we may point out a few features: (i) understandably, σ_R falls more steeply in the cases where the A–N transition is of first order character compared to the ones where it has a second order nature; (ii) for a wide range of compositions (between 76.8% to 44.6% NPOOB), σ_R value shows a broad minimum at $T_{NI} - T \simeq 32°$ and starts *increasing* as the temperature is lowered further. The fact that

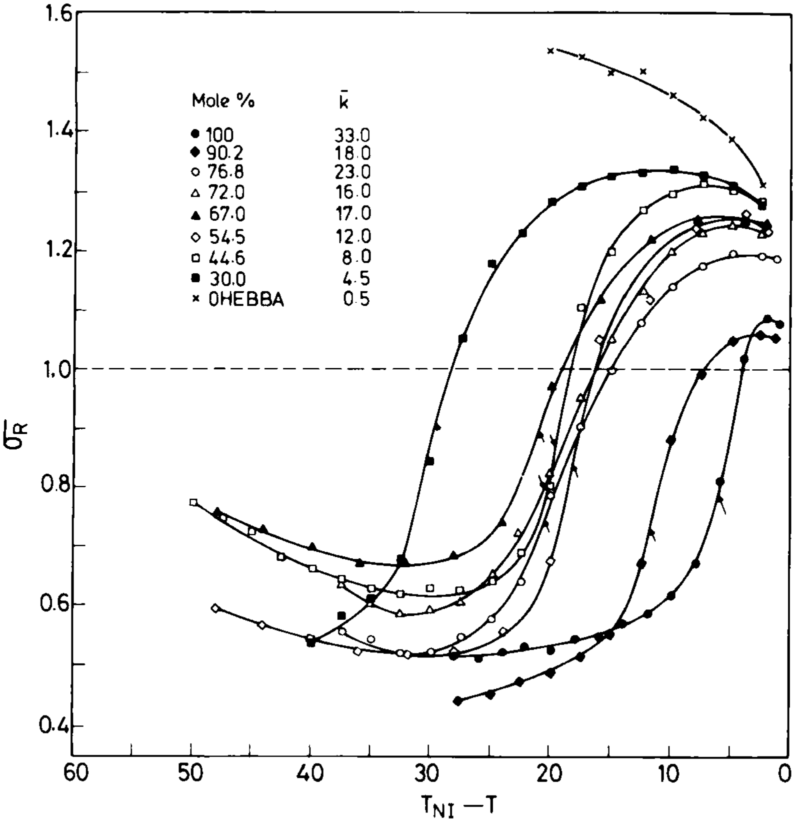

FIGURE 17 The ratios of the principal conductivities $\sigma_R = \sigma_\parallel/\sigma_\perp$ of various mixtures of NPOOB with OH-EBBA as functions of relative temperature. The first number against each symbol is the mole percentage of NPOOB and the second number the mean specific conductivity $\bar{K} \times 10^9$ $(\Omega \cdot \mathrm{cm})^{-1}$ at 76°C. The arrows indicate T_{AN}.

the A–N transition is very weak for the composition corresponding to the minimum in the A–N boundary and becomes stronger on either side of this composition is reflected in the cross over temperature (T_{Cr}) of the conductivity anisotropy. As seen in Figure 18, $T_{Cr} - T_{AN}$ shows a strong peak for the composition corresponding to the minimum in the A–N boundary, since the smectic-like short range order fluctuations are very strong in this case even at temperatures a few degrees above T_{AN}.

In conclusion, the competition between two types of interactions, *viz.*, charge transfer complex formation between the highly polar and weakly

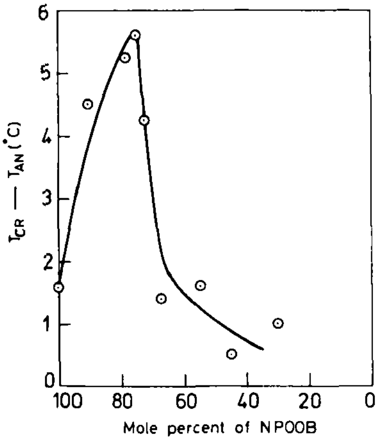

FIGURE 18 Composition-dependence of the relative crossover temperatures of the conductivities of mixtures of NPOOB with OH-EBBA.

polar molecules and the antiparallel interaction between the highly polar molecules gives rise to some interesting physical properties of the mixtures that we have studied.

Acknowledgments

We are grateful to Professor S. Chandrasekhar for some useful discussions. Our thanks are also due to Dr. K. A. Suresh for help with the X-ray studies.

References

1. H. Sackmann and D. Demus, *Z. Phys. Chem. (Leipzig)*, **224**, 177 (1963).
2. J. S. Dave, K. L. Patel and K. L. Vasanth, *Indian J. Chem.*, **4**, 505 (1966).
3. G. Pelzl, D. Demus and H. Sackmann, *Z. Phys. Chem. (Leipzig)*, **238**, 22 (1968).
4. J. W. Park, C. S. Bak and M. M. Labes, *J. Am. Chem. Soc.*, **97**, 4398 (1975).
5. C. S. Oh, *Mol. Cryst. Liq. Cryst.*, **42**, 1 (1977).
6. A. C. Griffin, R. F. Fisher and S. J. Havens, *J. Am. Chem. Soc.*, **100**, 6329 (1978).
7. K. P. L. Moodithaya and N. V. Madhusudana, in Liquid Crystals, Proceedings of the International Conference on Liquid Crystals, Bangalore 1979, Ed. S. Chandrasekhar (Heyden, London, 1980) p. 297.
8. F. Schneider and N. K. Sharma, *Z. Naturforsch.*, **36a**, 62 and 1086 (1981) and references given therein.
9. J. Szabon and I. Janossy, in Ad. Liq. Cryst. Res. Appl. Ed. L. Bata (Oxford, 1980) p. 229.
10. J. Szabon and S. Diele, *Cryst. Res. Technol.*, **17**, 1315 (1982).
11. N. K. Sharma, G. Pelzl, D. Demus and W. Weissflog, *Z. Phys. Chem. (Leipzig)*, **261**, 579 (1980).
12. M. Fukai and Y. Matsunaga, *Bull. Chem. Soc. Japan*, **54**, 3137 (1981).

13. A. J. Leadbetter, J. C. Frost, J. P. Gaughan, G. W. Gray and A Mosley, *J. de Physique*, **40**, 375 (1979).
14. N. V. Madhusudana and S. Chandrasekhar, Proc. Int. Liquid Crystals Conf., Bangalore 1973, Pramana Suppl. **1**, p. 57.
15. B. Engelen, G. Heppke, R. Hopf and F. Schneider, *Mol. Cryst. Liquid Cryst. Lett.*, **49**, 193 (1979).
16. G. Sigaud, F. Hardouin, M. F. Achard and H. Gasparoux, *J. de Physique*, **40**, C3-356 (1979).
17. P. E. Cladis, D. Guillon, W. B. Daniels and A. C. Griffin, *Mol. Cryst. Liquid Cryst. Lett.*, **56**, 89 (1979).
18. A. M. Levelut, R. J. Tarento, F. Hardouin, M. F. Archard and G. Sigaud, *Phys. Rev.*, **A24**, 2180 (1981).
19. M. I. Barnik, S. V. Belyaev, V. G. Rumyantsev, V. A. Tsvetkov and N. M. Shtykov, Forschungen Über Flussige Kristalle, Ed. D. Demus, Martin-Luther-University, Halle (1978), p. 84.
20. L. Bata and A. Buka, *Acta Phys. Polon.*, **A54**, 635 (1978).
21. G. J. Sprokel, *Mol. Cryst. Liquid Cryst.*, **42**, 233 (1977).
22. A. Mircea-Roussel, L. Leger, F. Rondelez and W. H. de Jeu, *J. de Physique*, **36**, C1-93 (1975).
23. F. Rondelez, Contribution a l'etude des effects de champs dans les cristaux liquides nematiques et cholesteriques, Ph.D. Thesis, University of Paris-Sud, Orsay (1973).
24. F. Schneider, *Z. Naturforsch.*, **33a**, 601 (1978).